# PEDOGENESIS ALONG A CLIMOSEQUENCE IN LOESS-DERIVED SOILS OF THE CENTRAL GREAT PLAINS

By

Scott Thomas Klopfenstein

Submitted to the graduate degree program in Geography and the Graduate Faculty of the University of Kansas in partial fulfillment of the requirements for the degree of Master of Arts.

_____

Chairperson William C. Johnson, Ph.D.

_____

Co-Chairperson Daniel R. Hirmas, Ph.D.

_____

Stephen L. Egbert, Ph.D.

Date Defended: 4/3/2014

The Thesis Committee for Scott Thomas Klopfenstein

certifies that this is the approved version of the following thesis:

PEDOGENESIS ALONG A CLIMOSEQUENCE IN LOESS-DERIVED SOILS OF THE CENTRAL GREAT PLAINS

_____

Chairperson William C. Johnson, Ph.D.

Date approved: 4/3/2014

## ABSTRACT

Understanding the pedogenic effects of average annual precipitation on loess-derived soils provides insight to past climate scenarios based on buried paleosols, as well as the ability to better predict future soil morphological changes due to projected climate forcings. This study explains variability in soil morphological properties in surface loess along a precipitation gradient in the Central Great Plains of the United States. Soil cores were collected from undisturbed portions of seven pioneer cemeteries to a depth of 50 cm across the transect spanning northwest Kansas into western Missouri. Pioneer cemeteries were selected due to the likely undisturbed nature of the soils in unused portions of the cemeteries. Soil cores were cut into 2.5-cm intervals, which were prepared and analyzed for bulk density (BD), color (CIELAB 1976 color space), organic carbon (OC) obtained from a modified Walkley-Black method, and aggregated and disaggregated particle-size distributions (PSD) from laser diffraction. The predictor variables—annual precipitation, depth, and PSD—were used in multivariate analyses to explain the distribution of the pedogenic indicators: color, OC, BD, and complexed organic carbon (COC). Lightness (L*), OC, BD, and COC—an indicator of soil physical quality—were all significantly explained by average annual precipitation. A proxy for microaggregation, geometric mean shift (GMS), was developed for this study deriving the difference between the geometric mean of the untreated and pretreated PSD results. Microaggregation occurred below an OC to clay ratio of 0.163 in the upper 50 cm of the loess-derived soils analyzed in this study. Among the morphological variables considered, COC had the highest coefficient of determination ($R^2$ = 0.871) and BD was best explained by average annual precipitation. These findings indicate any future climate forcings resulting in precipitation changes may have an effect on soil physical quality of loess-derived soils.

## ACKNOWLEDGEMENTS

I am very grateful for the encouragement, guidance, and funding provided by my advisor Dr. William C. Johnson. This work could not have been accomplished without the countless hours invested by Dr. Daniel R. Hirmas, every step of the way, from experimental design, to laboratory analysis, and writing. This project was funded in part by a Kollmorgen Graduate Research Scholarship from the Univeristy of Kansas, Department of Geography. Data used for the timing and magnitude of precipitation in this study were provided by Dr. Nathaniel Brunsell and Cassie Wilson. The Geological Society of America South-Central Section generously provided funding, in part, to showcase this work in a poster presentation at the 2013 Geological Society of America annual meeting in Denver, CO. Lastly, I am deeply appreciative of my wife, parents, and children for their constant support and unwavering faith and love permitting this project to come to fruition.

## TABLE OF CONTENTS

**ABSTRACT**…….. iii

**ACKNOWLEDGEMENTS**……..iv

**TABLE OF CONTENTS**…….. v

**CHAPTER 1. INTRODUCTION**……..1

**CHAPTER 2. MATERIALS AND METHODS**……..……5
*Study Area* ……...…5
*Soil Sampling and Analyses* ……8

**CHAPTER 3. RESULTS**…….....13
*Climate Variability*…….13
*Soil Color*……...……13
*Bulk Density*……...……15
*Organic Carbon*……17
*Particle-Size Distribution*……..…….……... 22

**CHAPTER 4. DISCUSSION**……..…… 24
*Organic Carbon-Clay Ratios, Complexed Organic Carbon, and Soil Aggregation*….…… 24
*Pedogenic Implications for Loess-Derived Soils*……...……....28

**CHAPTER 5. CONCLUSIONS**……...……...……36

**REFERENCES**…….……38

# CHAPTER 1. INTRODUCTION

Loess deposits are widely distributed in the conterminous United States and are, on average, thicker than in most other locations on Earth (Bettis et al., 2003). Throughout the late Quaternary, this silt-dominated sediment periodically blanketed large areas with various rates of deposition affecting soil development (Jacobs and Mason, 2005). Loess serves as the parent material for large portions of the highly productive soils found in the Central Great Plains of North America. Understanding the effects of climate on pedogenesis in loess provides valuable insight into paleoenvironments during periods of stability and soil development, the record of which has been captured in buried soils (paleosols) preserved within the loess (Jacobs and Mason, 2005). Conversely, this information also provides a better ability to predict future soil morphological changes due to projected climate forcings.

Increasing quantity and frequency in the amount of annual precipitation tend to produce greater net primary production and litter input to the soil system until a maximum is reached, leading to greater soil organic carbon accumulation (Sala et al., 1988; Zhou et al., 2009). Sampling along a climosequence with systematically varying average annual precipitation has allowed for the ability to analyze the effects of precipitation on vegetation and soil properties (Burke et al., 1989; Hontoria et al., 1999; Zhou et al., 2009; Khormali and Kehl, 2011; Saiz et al., 2012). Tan et al. (2004) showed parent material and slope are important controls on soil organic carbon (SOC) distribution in surface soils making them important factors to consider in the design of climosequence studies. For instance, in a comparative study from Arkansas, Brye et al., 2004 found no statistically significant differences in soil OC between two precipitation regimes. Their climosequence, however, did not control for parent material, which may have masked the effect of precipitation on OC distribution. By contrast, other studies have shown that

average annual precipitation accounts for large amounts of the variability in SOC distribution (e.g., Saiz et al., 2012).

The complexity of natural systems makes it difficult to generalize soil behavior over large regions and is responsible for hiding the true nature of the effects of precipitation variables upon SOC storage in many studies aiming to explain organic carbon patterns across the landscape. Variance in other soil forming factors is a common problem researchers encounter when setting up comparisons of climatic effects on SOC storage in surface soils. Increases in precipitation tend to favor SOC accumulation due to greater biomass input, while an increase in temperature tends to decrease SOC accumulation due to both greater soil microbial activity and less effective moisture (Burke et al., 1989; Hontoria et al., 1999). Controlling for all other soil forming factors provides the ability to assess soil properties along a climosequence as to reveal the soil morphological impact of precipitation.

This study aims to explain the variability of morphological properties in loess-derived soils as a function of average annual precipitation in the Central Great Plains of the United States. The Central Great Plains provides a unique opportunity to reasonably control temperature, geomorphic setting, and parent material to sample soils within a consistent parent material over a relatively large precipitation gradient. In this region, precipitation and evapotranspiration strongly influence vegetation distribution, which in turn affects SOC storage. In general OC stocks become greater with increasing precipitation, making this an ideal region to study the effects of climate change on the soil carbon cycle (Koch et al., 1995). Sample locations were selected within the boundaries of pioneer cemeteries along an east-west precipitation gradient in order to increase the likelihood of the soil being undisturbed by European settlement in the 1800s. These sites were also similarly managed, typically with a combination of burning

and mowing throughout recent history. The objective of this study is to determine the effects of average annual precipitation on the pedogenic indicators—OC, bulk density, soil color, and soil aggregation—in near surface depths (0 – 50 cm) of soils formed in loess.

## CHAPTER 2. MATERIALS AND METHODS

*Study Area*

Seven pioneer cemeteries along an east-west precipitation gradient from northwest Kansas to western Missouri were sampled to investigate the effects of precipitation on soil morphological properties (Fig. 1; Table 1). These seven cemeteries were selected from a list of pioneer cemeteries established prior to 1906 compiled from a number of sources. Cemetery names were cross-referenced with the U.S. Board on Geographic Names (http://geonames.usgs.gov/) to obtain coordinate locations confirmed with National Agriculture Imagery Program (NAIP) imagery and U.S. Geological Survey Digital Raster Graphic files compiled into an ESRI shapefile (ESRI, Redlands, Ca) available on the Kansas Data Access and Support Center website (Johnson and Klopfenstein, 2013; DASC: http://www.kansasgis.org). Two additional cemeteries were included in this study—Mount Calvary and Allen Cemeteries—although not identified in available sources, but rather were discovered through field reconnaissance, and contained headstones with dates confirming the cemetery's establishment prior to the end of the 19th century. To further confirm the history of these sites, county plat books and atlases were consulted. Gettis, Leasburg, Mount Calvary, and Denton were all well documented in these sources. Reiter was not present in the county atlas or plat book; it was, however, referenced in other sources. Based on the cemetery symbol for Chardon in the 1906 Rawlins County plat book, the area sampled may have been an addition. The area sampled from Allen Cemetery also appears to be slightly outside the bounds of the original cemetery indicated in the 1877 Historical Atlas of Buchanan County, MO.

In order to control for differences in parent material and relief, only cemeteries sited on the upland mantle were selected in this study. Soil survey data accessed through the Natural

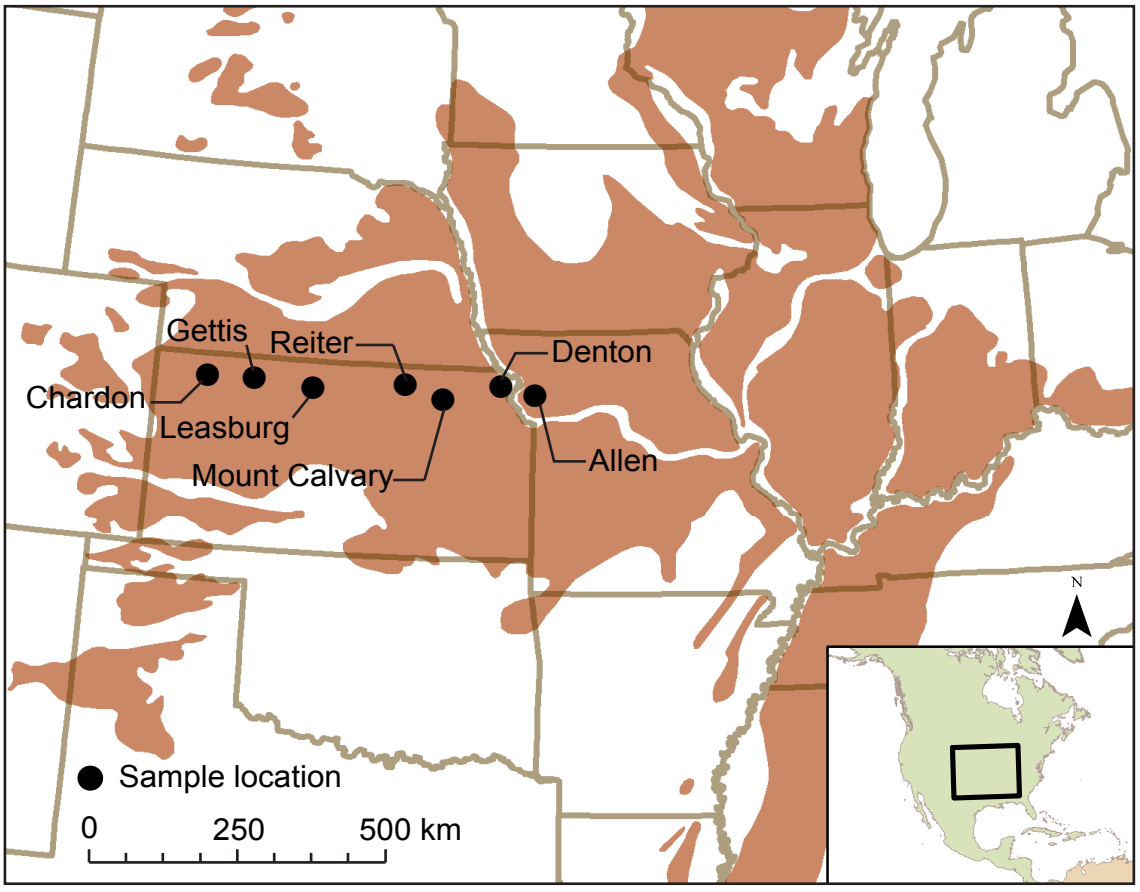


**Fig. 1.** Location of sample sites used in this study. Reddish-brown shaded areas show a generalized surface loess accumulation >20 cm thick. Loess distribution map modified from Bettis et al. (2003).

**Table 1**

Selected characteristics for the sample sites used in this study. High and low temperatures are given as the average normal high and low temperatures for the months of July and January, respectively. Soil series classification and parent material were obtained from Web Soil Survey (http://websoilsurvey.sc.egov.usda.gov/).

| Site Name | Latitude (°) | Longitude (°) | County | Normal precip.[a] (cm $yr^{-1}$) | Precip. timing[b] (events $d^{-1}$) | Precip. magnitude[b] (mm $event^{-1}$) | Average temp.[a] (°C) | High temp.[a] (°C) | Low temp.[a] (°C) | Soil classification | Soil series | Parent material | Notes |
|---|---|---|---|---|---|---|---|---|---|---|---|---|---|
| Chardon | 39.6618 | -101.0385 | Rawlins, KS | 53.2 | 0.171 | 7.80 | 10.8 | 31.6 | -8.8 | Fine-silty, mixed, superactive, mesic Aridic Argiustolls | Keith silt loam | Fine-silty loess | |
| Gettis | 39.6811 | -100.1334 | Norton, KS | 57.1 | 0.179 | 8.23 | 11.1 | 31.3 | -8.7 | Fine-silty, mixed, superactive, mesic Typic Argiustolls | Holdrege silt loam | Calcareous loess | Does not appear to be original vegetation, border shrub roots found in cores |
| Leasburg | 39.5819 | -98.9734 | Smith, KS | 66.0 | 0.190 | 8.83 | 11.5 | 32.0 | -8.5 | Fine, smectitic, mesic Typic Argiustolls | Harney silt loam | Loess | Avoided trees |
| Reiter | 39.7112 | -97.1533 | Washington, KS | 79.3 | 0.214 | 9.37 | 11.7 | 31.0 | -7.8 | Fine, smectitic, mesic Udic Argiustolls | Longford silt loam | Silty and clayey loess over loamy pedisediment | Area sampled was hayed 2013 |
| Mount Calvary | 39.4874 | -96.4088 | Pottawatomie, KS | 87.2 | 0.225 | 9.72 | 11.9 | 30.8 | -7.6 | Fine, smectitic, mesic Oxyaquic Vertic Argiudolls | Pawnee clay loam | Clayey drift | Area sampled was burned 2012 |
| Denton | 39.7265 | -95.2844 | Doniphan, KS | 92.5 | 0.227 | 10.33 | 11.7 | 29.9 | -7.2 | Fine, smectitic, mesic Typic Argiudolls | Aksarben silty clay loam | Loess | NW corner possibly disturbed (avoided), railroad passed through SE corner |
| Allen | 39.6025 | -94.6022 | Buchanan, MO | 98.1 | 0.232 | 10.64 | 11.9 | 29.8 | -6.8 | Fine-silty, mixed, superactive, mesic Typic Hapludolls | Marshall silt loam | Loess | Does not appear to be original vegetation (clover) |

[a] Precip. = precipitation; temp. = temperature. Interpolated from regional stations with available normal values from 1981-2010 (NCDC).

[b] Interpolated from regional stations with at least 80 consecutive years of precipitation data available (USHCN).

Resources Conservation Service (NRCS) were used to identify loess parent material at each site (http://websoilsurvey.sc.egov.usda.gov/) (Table 1). One exception was the Mount Calvary Cemetery which was described as clayey drift; however, no erratics were present in the depth interval sampled, and the texture was similar to other sites along the transect, which had soils described as loess-derived. Slopes at the sites ranged from 0 to 10% as measured with a field clinometer.

Other factors considered in site selection were latitudinal range, sampling accessibility, and level of disturbance (Table 1). Only cemeteries within the range of 39°N to 40°N were considered in order to limit variation in temperature as well as to avoid surface effects of the 1930's Dust Bowl, which deposited thick layers of modern aeolian dust farther south in Kansas. Aerial imagery was viewed to determine accessibility to cemetery sites as well as grave density. If a cemetery vehicular access appeared too difficult or the density of graves left little or no area suitable for sampling, then it was excluded. Disturbance factors to be avoided during sampling were graves, spoil piles, tree rooting zones, and traffic areas (e.g., roads, paths, and tire ruts). Although an attempt was made to sample sites with native vegetation, two sites showed signs of probable disturbance based on the plant species and diversity present. Gettis Cemetery appeared to have been planted to cool season grasses and the area available for sampling at Allen Cemetery may have been an addition that was not originally platted with the cemetery; this addition was inferred from the dominance of clover in the vegetative cover.

*Soil Sampling and Analyses*

Three precipitation variables—annual precipitation, timing of events (average likelihood of a measurable event on any day of the year), and event magnitude (average amount of precipitation

per event)—were considered for this study. Timing and magnitude data were selected from a set of stations that had over 80 years of consecutive data (US Historical Climate Network, USHCN; http://cdiac.ornl.gov/epubs/ndp/ushcn/ushcn.html). The stations were plotted as points in ArcMap 10.1 (ESRI, Redlands, CA) based on the latitude and longitude provided. Values for timing and magnitude were interpolated using empirical Bayesian kriging in ArcMap with a cell size equivalent to half the average distance between pairs of stations in the dataset. Timing and magnitude data were then compiled for each sampling location from the interpolation. A similar process was conducted with average annual precipitation, which was derived from a set of weather stations reporting 30-year normals for the period 1981-2010 (National Climatic Data Center, NCDC; http://www.ncdc.noaa.gov/). Average annual temperature, average July high temperature, and average January low temperature were also extracted from 30-year normals for the period 1981-2010; however, a different set of weather stations was used due to availability of observations (NCDC; http://www.ncdc.noaa.gov/). Locations of weather stations used for each interpolation are shown in Fig. 2.

A hand corer (Soil Recovery Probe, AMS, American Falls, ID) was used to collect triplicate soil cores (2.23 cm diameter) to a depth of 50 cm. Cores were sampled in plastic lined tubes that were capped and transported to the University of Kansas (KU) Soils and Geomorphology Laboratory. Observations of vegetation, management, and history were gathered from field observation and aerial imagery. Representative samples were taken at locations that avoided disturbance features.

Cores from each site were carefully cut into 2.5-cm increments with a hand miter saw. Soil was then removed from each plastic tube segment and placed into a pre-weighed metal tin; negligible amounts of soil remained on the plastic tubing. After being weighed and dried for 12

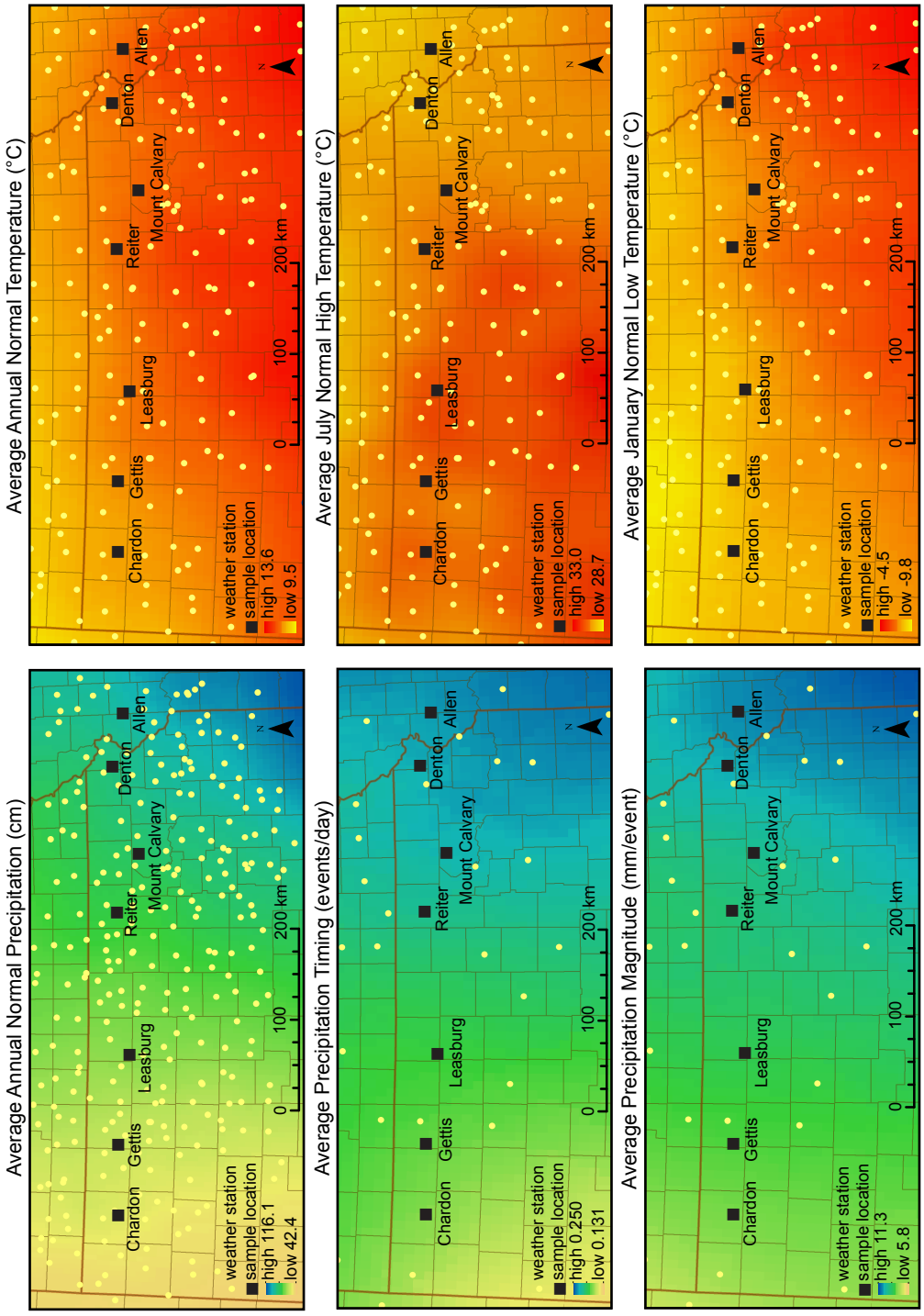


**Fig. 2.** Selected climate variables interpolated from weather stations with available data in the region. Cell size used for interpolation is half the average distance between stations for each dataset. Average annual precipitation and temperature values are 30-year normals 1981-2010 (NCDC). Average precipitation magnitude and timing are from stations that had at least 80 years of continuous data (USHCN).

hours at 60°C, samples were reweighed, gently ground with a ceramic mortar and pestle, and passed through a #20-mesh sieve (0.841 mm). A #20-mesh sieve was used to ensure homogeneity due to limited quantity of sample and to the necessity of performing multiple analyses with the small mass of sample available. Rocks and roots observed on the sieve were removed with tweezers and weighed and recorded. The mass of each sample was used to calculate bulk density after correcting for water content, rock fragments, and root mass (Blake and Hartge, 1986).

Samples were analyzed for organic matter (OM) using the heat-of-dilution modification of the Walkley-Black method (Combs and Nathan, 1998). These values were corrected for water content and converted to organic carbon (OC) using the established 1.72:1 OM:OC ratio (Burt, 2004). The Arrouays and Pelissier (1994) depth function was fit to OC values at each site. This model can be expressed as (Eq. 1):

$$C(z) = \frac{[\exp(-bz) - \exp(-bz_2)](C_1 - C_2)}{\exp(-bz_1) - \exp(-bz_2)} + C_2 \quad (1)$$

where, $C(z)$ is OC content at depth $z$, $z_1$ and $z_2$ represent the 1.25 cm and 48.75 cm depths, respectively, $C_1$ and $C_2$ are the OC contents at $z_1$ and $z_2$, respectively, and $b$ is a fitting parameter that represents the rate of change of OC with depth (Arrouays and Pelissier, 1994; Bernoux et al., 1998).

Dried ground samples were placed into testing wells on a plastic tray designed to isolate and moisten aliquots during color analysis. Soil colors were determined in the CIE 1976 (L*a*b*) space (CIE, 1978) for moist samples using a reflectance spectrophotometer (CM700D, Konica Minolta, Tokyo, Japan). In the CIE 1976 space, L* values represent lightness—values range from 0 (black) to 100 (white). Values on the a* scale move from green (-) to red (+) and values on the b* scale move from blue (-) to yellow (+) (Torrent and Barrón, 1993).

A representative core was selected from each site for particle-size distribution (PSD) analysis. These cores were sampled at 10 evenly-distributed depth intervals between 0 and 50 cm. Two subsamples were taken from each depth interval to examine the effect of OC on aggregate-size distribution. Inorganic carbon content was minimal in all samples as inferred from the absence of reaction with 10% HCl; thus, samples were not pretreated for carbonate. One subsample from each depth was pretreated to remove OC while the other was left untreated. Pretreatment was conducted following a modified procedure from Burt (2004). Two mL of 30% $H_2O_2$ was added to 0.5 g of sample and heated to 90°C until reaction was no longer observed, but no less than 30 min. Samples were washed with deionized water (DI) and volumes reduced by centrifugation; samples were resuspended in 20 mL of DI. This treatment was intended to remove the OC that was aggregating mineral particles. PSD from pretreated and untreated samples were determined in a water suspension by laser diffractometry (Mastersizer 2000, Malvern Instruments, Worcestershire, UK). The difference between geometric means of pretreated and untreated PSDs was used as a proxy for aggregation and defined here as geometric mean shift (GMS):

$$\mathrm{GMS} = \mathrm{GM}(d_i^u) - \mathrm{GM}(d_i^p) \quad (2)$$

where, GM represents the geometric mean, $d_i^u$ is the set of particle diameters from the laser diffractometer for an untreated sample, and $d_i^p$ is the set of particle diameters for a pretreated sample.

All statistics, including tests of significance, simple and multivariate regressions, transformations, parameter and beta-weight estimations, and graphics were analyzed using R 2.14.2 (R Development Core Team, Vienna, Austria). GMS was plotted as a function of OC:clay

ratio and fit with a broken-stick linear regression model using the ‘segmented’ package for R (Muggeo, 2008).

# CHAPTER 3. RESULTS

*Climate Variability*

Average annual precipitation values increase from 53.2 cm $yr^{-1}$ on the western end of the transect at Chardon Cemetery to 98.1 cm $yr^{-1}$ on the eastern end at Allen Cemetery (Table 1). Timing of precipitation events follows a similar trend with lower frequencies observed to the west (0.171 events $d^{-1}$ at Chardon) and higher frequencies observed in the east (0.232 events $d^{-1}$ at Allen). Precipitation magnitude also increases toward the east, ranging from 7.8 mm $event^{-1}$ at Chardon to 10.6 mm $event^{-1}$ at Allen (Table 1). Average temperatures exhibit minimal variation, ranging from 10.8 to 11.9°C from west to east, respectively. Average July high temperatures also display minimal variation from 29.8 to 32.0°C; average January low temperatures range from -8.8 to -6.8°C across the transect (Table 1).

*Soil Color*

Color lightens below 10 cm for all sites, except Chardon, as indicated by increasing L* values (Fig. 3). Average lightness for Chardon increases only slightly below 45 cm. Mount Calvary exhibits a more rapid transition with depth to higher L* values between approximately 12 and 18 cm; L* values increase gradually beyond that point. Western sites, which have lower average annual precipitation, show greater variation among representative cores below 20 cm as indicated by standard deviations. Allen cemetery, which occurs farthest east along the transect, also generally indicates a slight increase in variation with depth below 25 cm. Thus, with the exception of Allen Cemetery, the drier sites reveal greater variation with depth than those with greater average annual precipitation, as indicated by standard deviation.

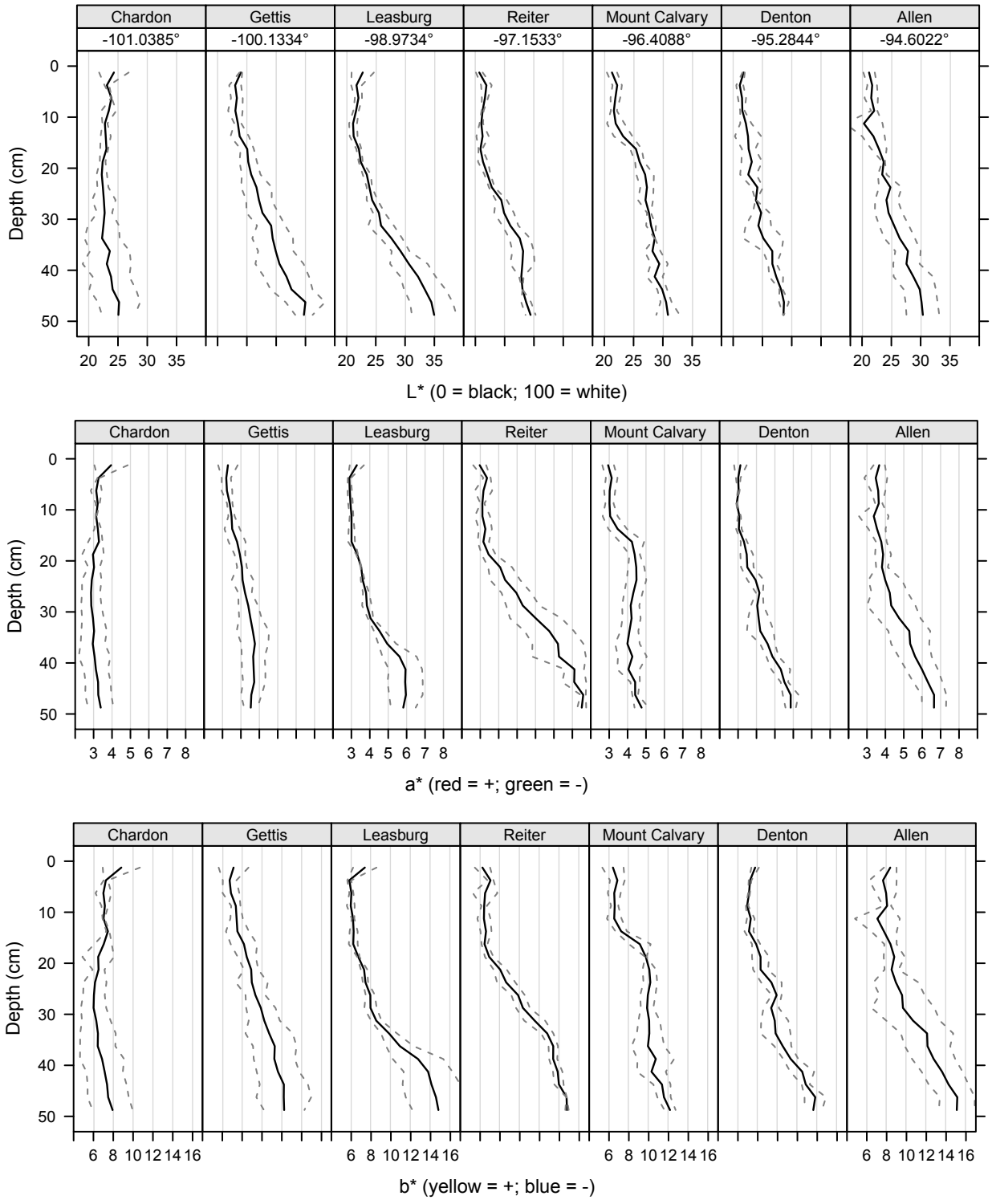


**Fig. 3.** Moist L*, a*, and b* depth profiles for each site studied. L*, a*, and b* are based on the Delta E dimension for determining the difference between two color tones. Delta E is the smallest perceptible unit. Solid lines correspond to mean values obtained from 3 cores; dashed lines represent ±1 standard deviation about the mean values. Sites are ordered from west to east across the transect.

Rubification (a* values) begins to increase between 10 and 20 cm for all plots except Chardon and Gettis (i.e., the two driest sites; Fig. 3). Chardon shows no appreciable increase in rubification, while Gettis shows only a slight increase with depth over 50 cm. As with L* values, Mount Calvary displays a sharp jump in rubification between 12 and 18 cm and remains relatively constant below that depth. Leasburg has a similar jump in rubification deeper in the profile between 30 and 40 cm. Below 35 cm, Reiter exhibits the highest rubification values for any of the sites. Leasburg, Reiter, and Allen have the largest variation in rubification values with depth; Reiter has a decrease in variation below 45 cm.

All sites are characterized generally by increasing b* values (yellowness) with depths below 10 cm (Fig. 3). Chardon has the smallest increase among the sites. As with a* values, Mount Calvary and Leasburg display an increase in b* values between 12-18 cm and 30-40 cm, respectively. Chardon, Gettis, Leasburg, and Allen present the greatest variability with depth among the sites.

*Bulk Density*

Average bulk density for the surface depth (0 – 2.5 cm) ranges from 0.87 g $cm^{-3}$ at Chardon to 1.07 g $cm^{-3}$ at Mount Calvary (Fig. 4). These surface samples contain varying thicknesses of plant litter, which likely contribute to the low bulk density values. At depth (47.5 – 50 cm) the values for bulk density range from 1.10 g $cm^{-3}$ at Chardon to 1.43 g $cm^{-3}$ at Reiter. The eastern sites generally have slightly higher bulk densities deeper in the profile. Chardon has a relatively low and constant bulk density below about 5 cm, never increasing past 1.14 g $cm^{-3}$ in the upper 50 cm. Most sites display a linear increase of bulk density with depth, while Chardon,

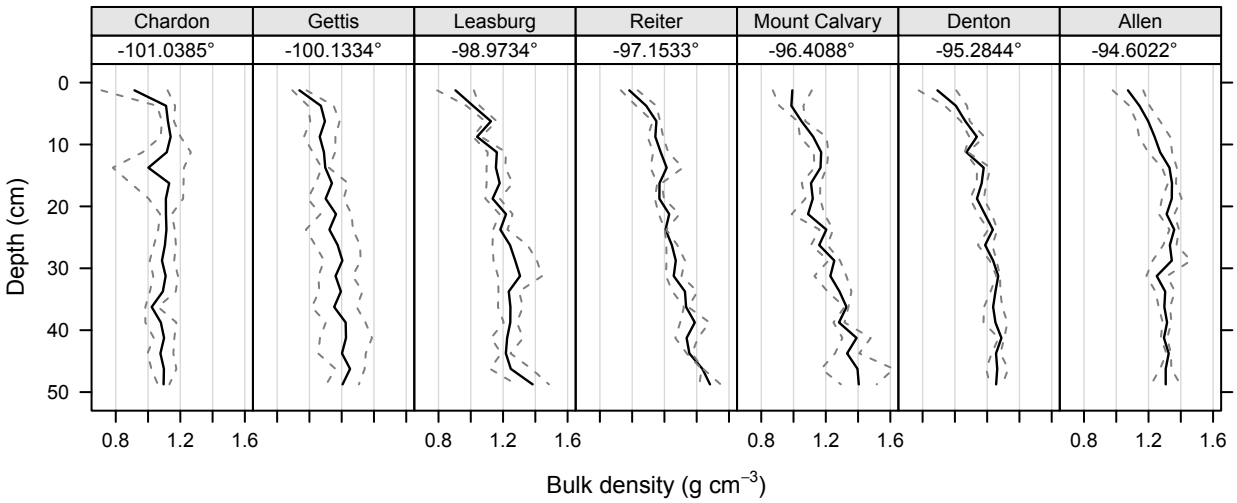


**Fig. 4.** Bulk density depth profiles for each site studied. Solid line corresponds to mean values obtained from 3 cores; dashed line represents ±1 standard deviation about the mean values. Sites are ordered from west to east across the tranasect.

Denton, and Allen seem to asymptotically reach their deepest values. Based on their standard deviations, the highest variation among replicates occurs at Chardon and Gettis (Fig. 4).

*Organic Carbon*

Soil organic carbon (OC) values decrease exponentially with depth at all sites, as expected (Fig. 5). Surface OC values (0 – 2.5 cm) range from 3.5 to 4.4% OC, while the deepest OC values (47.5 – 50 cm) range from 0.6 to 1.2% OC. Depth profiles of OC indicate slightly larger variation at Chardon and Allen (the extreme ends of the transect) than at other sites; however, Denton cemetery exhibits a slightly wider variation in the upper 20 cm. Slopes from the exponential decay function (Eq. 1) fit to the OC depth profiles (i.e., rate of change of OC with depth) against average annual precipitation show a decreasing trend with increasing precipitation, indicating that OC is distributed deeper into the soil profile with higher precipitation (Fig. 6). Leasburg and Allen are outliers in that they portray a lower and higher rate of change with depth than predicted, respectively.

Total OC was converted to an areal basis by multiplying bulk density by the percentage of OC on a mass basis averaged for each depth interval (0 – 10, 10 – 20, 20 – 30, 40 – 50 cm). These values were plotted against average annual precipitation to examine the trend of total organic carbon across the transect (Fig. 7). Soil OC tends to increase with increasing average annual precipitation as indicated by the positive slope displayed for each depth interval examined. Thus, a positive correlation between OC and average annual precipitation exists throughout the surface 50 cm. These trends are indicated by the positive slopes of the best-fit linear regressions (Fig. 7; Table 2). The greatest slope appears in the 0-10 cm depth interval, indicating that the effects of average annual precipitation are being expressed most strongly near

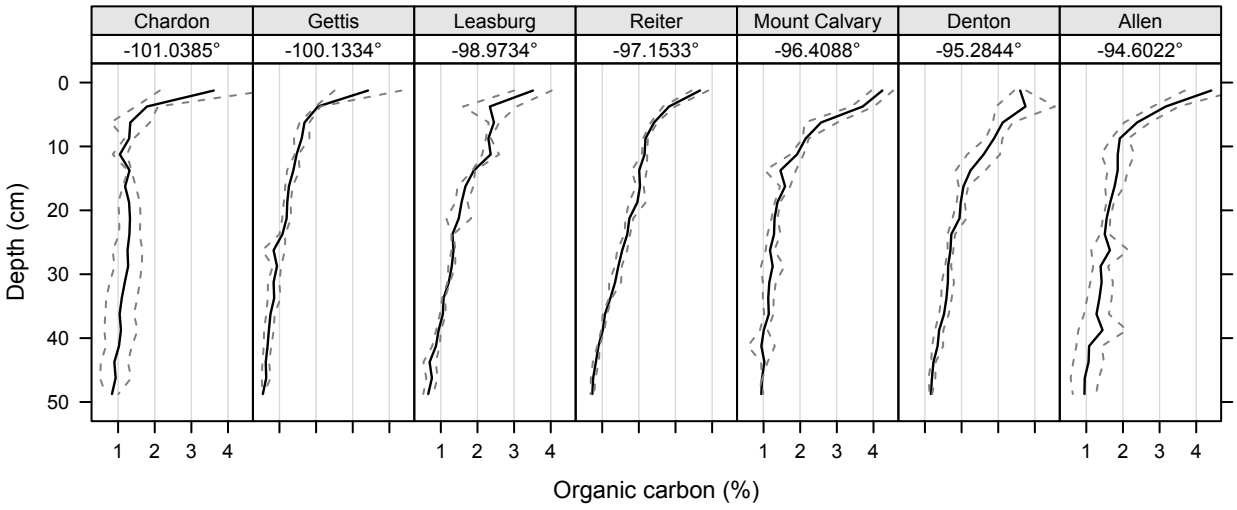


**Fig. 5.** Organic carbon depth profiles for each of the sites. Solid lines correspond to mean values obtained from 3 cores; dashed lines represent ±1 standard deviation about the mean values. Sites are ordered from west to east across the transect.

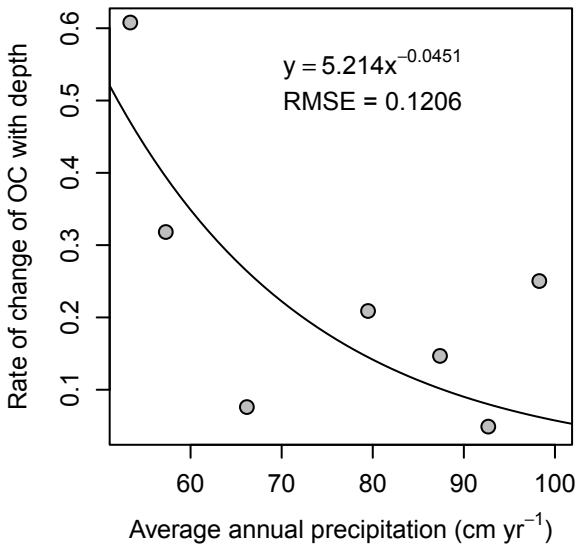


**Fig. 6.** Slope of the OC depth profile as a function of average annual precipitation.

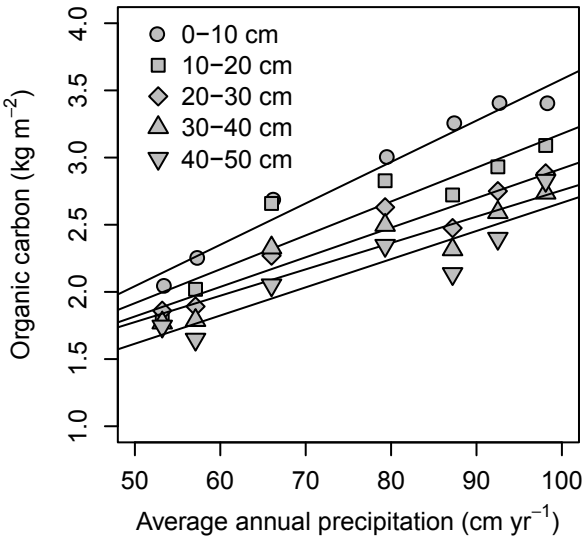


**Fig. 7.** Total OC for each 10-cm depth interval against average annual preciptation.

**Table 2**

Coefficients and $r^2$ values from the regression of precipitation and total OC for each of the 10-cm depth intervals. Values following coefficient estimates represent the standard errors.

| Depth interval (cm) | Slope | Intercept | $r^2$ |
|---|---|---|---|
| 0-10 | 0.0308±0.0024 | 0.502±0.190 | 0.963 |
| 10-20 | 0.0252±0.0048 | 0.655±0.373 | 0.847 |
| 20-30 | 0.0220±0.0028 | 0.716±0.216 | 0.927 |
| 30-40 | 0.0196±0.0038 | 0.794±0.297 | 0.841 |
| 40-50 | 0.0210±0.0042 | 0.566±0.325 | 0.835 |

the surface (Table 2). Coefficient of determination ($r^2$) values range from 0.835 to 0.963 and indicate that average annual precipitation explains most of the variation in OC for all depth intervals analyzed. The intercepts range from 0.502 to 0.794 and tend to increase with the exception of the 40-50 cm depth interval (Table 2). Deeper in the profile (i.e., all ranges below 0 – 10 cm) the OC values reach a peak at Reiter (79.3 cm $yr^{-1}$), decline at Mount Calvary (87.2 cm $yr^{-1}$), and increase toward the east with increasing precipitation. Even when Mount Calvary is excluded, a plateau can be observed in the OC values for all depth intervals besides 0 – 10 cm from Reiter (79.3 $cm^{-1}$) to Denton (92.5 cm $yr^{-1}$).

*Particle-Size Distribution*

Average clay content along the transect was approximately 10% and exhibits little variability with either depth or site (Fig. 8). Silt was the largest fraction of the particle-size distribution at each site, further confirming that the soils were formed in silt-dominated loess. The silt fraction for all depth intervals and at all sites ranges between slightly below 60% to just over 80%. Silt content generally increases from west to east along the transect whereas the variability of silt content with depth decreases. The reverse trend occurs with sand content, which decreases from the western end of the transect to the eastern end (Fig. 8). However, as with silt content, the variability of sand content with depth generally decreases from west to east.

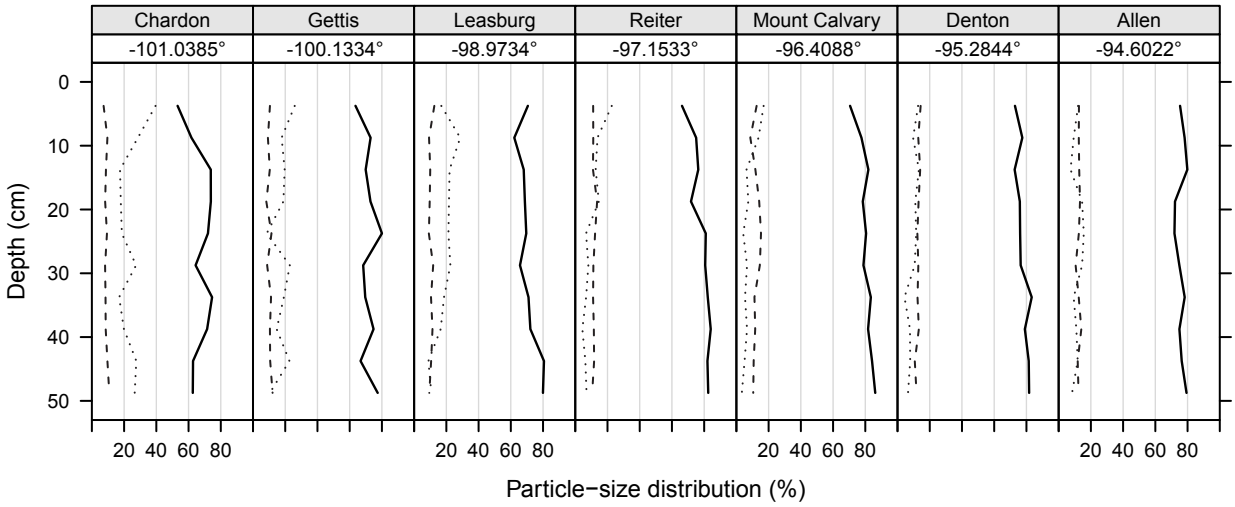


**Fig. 8.** PSD profiles for each site studied. Lines represent sand (dotted), silt (solid), and clay (dashed) content obtained from the representative core. Sites are ordered from west to east across the transect.

## CHAPTER 4. DISCUSSION

*Organic Carbon-Clay Ratios, Complexed Organic Carbon, and Soil Aggregation*

Variations in parent material and drainage have been shown to have significant influence on soil development (Tan et al. 2004). Controlling parent material in this study permitted the isolation of precipitation as the primary independent variable affecting soil development among the sites studied. Depth profiles indicated that OC decreased westward along the transect (i.e., with decreasing precipitation; Fig. 5) as reported in other climosequence and loess investigations (e.g., Burke et al., 1989; Hontoria et al., 1999; Khormali and Kehl, 2011). The tight coupling between SOC at the surface compared to other depths (Fig. 7) strongly suggests that precipitation is controlling the amount of OC through its effect on net primary production (Sala et al., 1988; Jobbágy and Jackson, 2000). Although there are too few sites along the transect to obtain more confidence in the character of the relationship, the data suggest that OC may be better predicted from precipitation using an asymptotic model (Fig. 7). The upper four depth intervals (i.e., 0 – 40 cm) in Fig. 7 appear to especially show this asymptotic trend of increasing OC with increasing precipitation. This trend is interpreted to indicate that a greater response in OC to increasing total annual precipitation should be expected for soils with drier climatic regimes (i.e., <75 cm $yr^{-1}$) compared to soils under more humid conditions (i.e., >75 cm $yr^{-1}$). Since the western sites are moisture limited compared to the eastern sites, these profiles tend to respond more strongly to increasing water availability. This observation is closely related to that of total litter mass, which has been shown to follow a quadratic equation increasing to about 90-95 cm $yr^{-1}$ (near the upper limit of this study) before beginning to decrease (Zhou et al., 2009). A stronger correlation of OC with average annual precipitation at shallow depths (<40 cm) compared to deeper depths (>50 cm) is likely due to the near-surface biomass inputs from litter and roots under temperate

grasslands (Jackson et al., 1996; Schulze et al., 1996; Jobbágy and Jackson, 2000). As shown in Fig. 6, a larger rate of change of OC with depth occurs on the drier end of the transect than in soils with greater rainfall, further illustrating the strong relationship between OC and precipitation.

Dexter et al. (2008) promoted the concept that complexed organic carbon (COC) controls aggregation in a soil. In their hypothesis, an OC:clay mass ratio of 0.1 represents a threshold found to predict soil COC. Below this threshold, COC was controlled by the total amount of OC in the soil whereas above this threshold, COC was controlled by the amount of clay in the soil. Several recent investigations have relied on COC as an indicator of soil physical quality because of its control on aggregation and because COC represents a sequestered pool of OC (Dexter et al., 2008; de Jonge et al., 2009; Eden et al., 2012). Soil physical quality is defined using the slope of the water retention curve at its inflection point as a proxy of microaggregate structure, which is indicative of the physical properties necessary to sustain ecosystem services such as plant productivity, water purification, water and nutrient retention, biodiversity, and others (Dexter, 2004). Subsequent researchers have discovered a range of OC:clay values near the 0.1 threshold, but suggest further research is necessary to better define this point (Schjonning et al., 2012; de Jonge et al., 2009).

In this study, new proxy for aggregation—GMS—was used to examine this threshold in loess soils. Figure 9 displays GMS values as a function of the ratio of OC:clay for all samples run for PSD analyses ($N$ = 70). This plot suggests that there are two domains describing the relationship between GMS and OC:clay ratio—one below an OC:clay ratio of approximately 0.15 where the GMS appears to be positively and linearly correlated with the ratio of OC:clay and another above that point where no obvious relationship appears between the variables (Fig.

9a). A broken-stick linear regression model was fit to the data to estimate the threshold between these two domains and yielded a breakpoint value of 0.163 with a standard error of 0.0412. This breakpoint is interpreted to mean that for the relatively undisturbed silt-dominated loess soils used in this study, every 1 g of OC was complexed with approximately 6 g of clay, as opposed to the 10 g of clay estimated from the water retention data in several Polish and French databases of agricultural soils used by Dexter et al. (2008). Below an OC:clay ratio of 0.163, the regression model illustrated in Fig. 9a explains 25.6% of the variation in GMS with a slope of 39.1 and intercept of 2.34. Although the amount of variation explained is modest, this regression is highly significant ($P < 0.001$) especially when compared to the model above this threshold, which explains only 3.2% of the variation in GMS and is not significant ($P = 0.545$).

Using this new OC:clay ratio of 0.163, COC was calculated for those samples with ratios less than this threshold as,

$$COC = OC \tag{3}$$

and for samples with ratios greater than 0.163 as,

$$COC = clay \times 0.163 \tag{4}$$

where OC, COC, and clay are given in percent on a mass basis (Dexter et al., 2008). In order to examine the relationship between aggregation and COC obtained with a threshold of 0.163, these two variables were regressed (Fig. 9b). The regression model explained slightly more (28.2%) of the variation in GMS than the OC:clay ratio alone (Fig. 9a) and was highly significant ($P < 0.001$) suggesting that, for loess soils, the new threshold is an improvement over the previously proposed 0.1 value. Comparisons and implications of using this new threshold are further discussed in the next section.

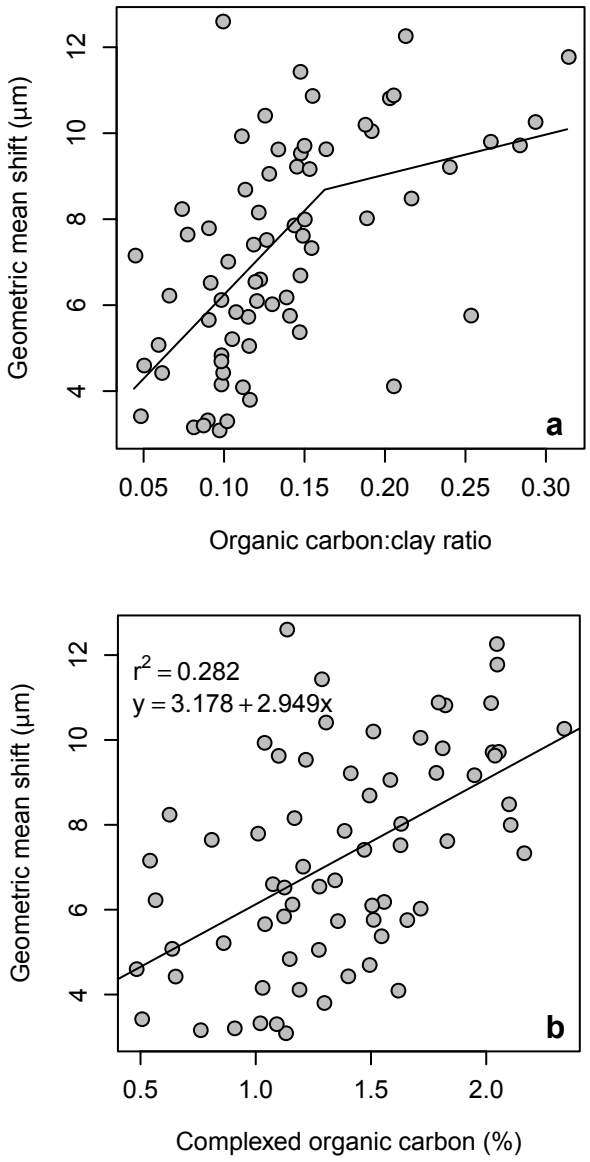


**Fig. 9.** (a) GMS as a function of OC:clay ratio. Lines represent a best-fit piecewise linear regression model. The breakpoint between the two lines is at an OC:clay value of 0.163. (b) GMS as a function of COC predicted using the OC:clay threshold of 0.163. The solid line represents a simple linear model fit to the data.

Complexed organic carbon depth profiles reveals several interesting trends (Fig. 10). In general, COC decreases with depth for all sites with the exception of a notable excursion near the bottom of the profile at Allen. This is likely due to an anomalous OC value from the core run for PSD at that depth (Fig. 5). Near the surface (0-5 cm), COC tends to increase from west (drier soil moisture) to east (more humid conditions) along the transect (Fig. 10). This was expected since there is a larger total amount of carbon at the surface as average annual precipitation increases toward the east (Figs. 5 and 7). Similarly, COC in the deepest layer increases from west to east (Fig. 10). Thus, both the upper and lower depths of the COC profile increase resulting in a generally linear depth distribution as depicted in Fig. 10. This distribution is different than the OC depth profiles (Fig. 5), which shows an exponential decrease with depth. Therefore, while there exists a tight coupling between surface OC abundance and precipitation for these soils, COC—which is a useful predictor of soil physical quality—is coupled to precipitation to at least 50 cm below the surface. Figure 11 illustrates this relationship by regressing total COC for the profile against average annual precipitation. Slope for the regression model is 0.119 ($P < 0.001$), and the intercept is not significantly different from zero ($P = 0.427$). Average annual precipitation explains 93.8% of the variation in total COC, which suggests that regional precipitation changes due to global climate forcings may contribute to the change of soil physical quality in loess in the upper 50 cm.

*Pedogenic Implications for Loess-Derived Soils*

In order to examine the pedogenic controls on soil morphology, multivariate regressions were run for OC, bulk density, color (i.e., L*, a*, b*), and COC separately against the predictor variables—annual precipitation, depth, and PSD (Fig. 12; Table 3). Specifically, these

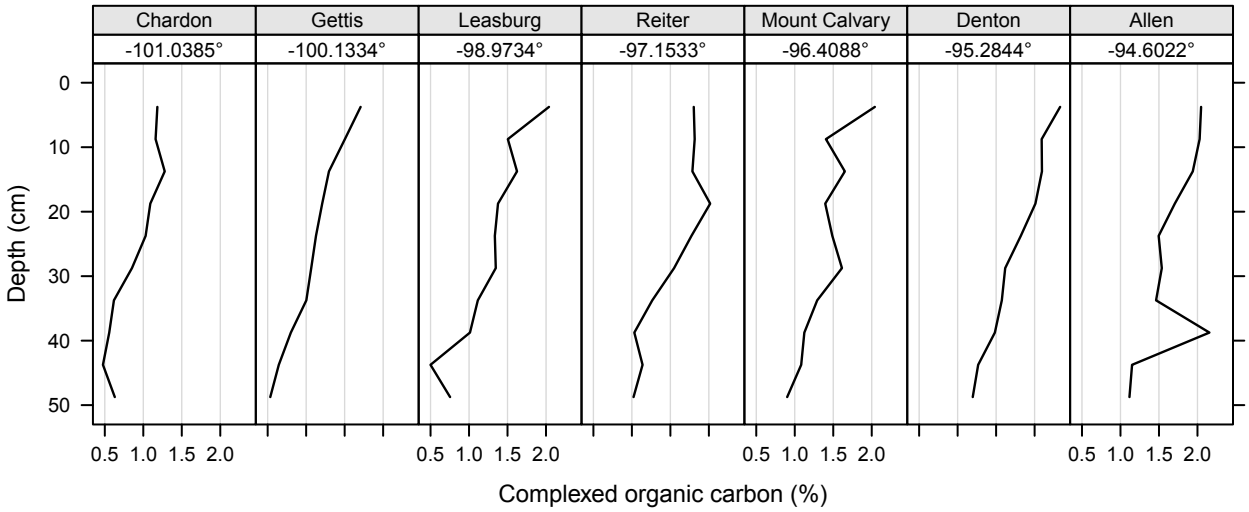


**Fig. 10.** COC profiles for each site along the transect. COC is represented by a solid line obtained from the threshold established in Fig. 9a. Sites are ordered from west to east across the transect.

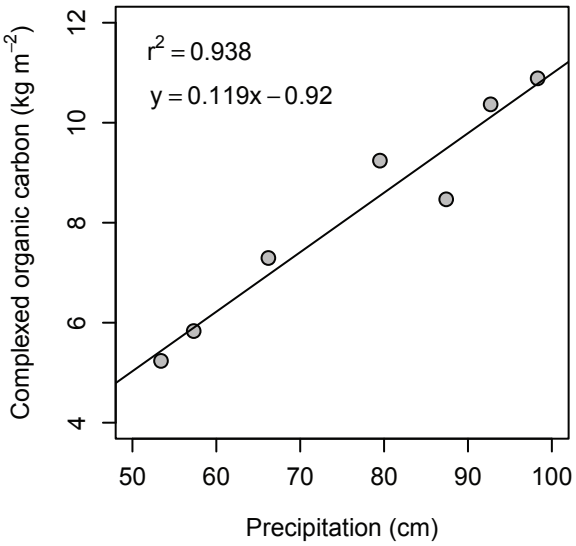


**Fig. 11.** Total COC for the entire 50-cm depth interval against average annual preciptation.

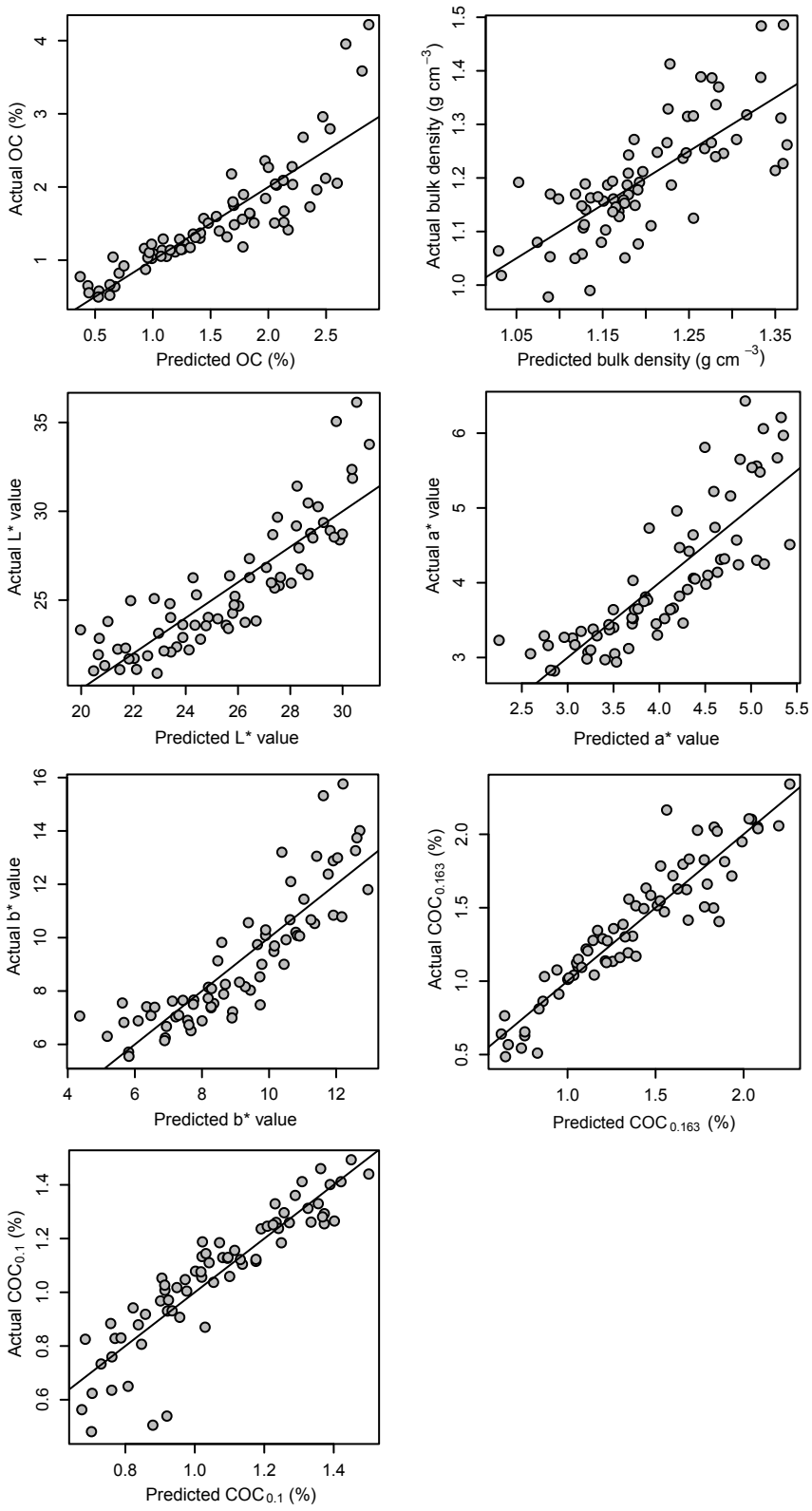


**Fig. 12.** Multivariate regression summary plots for the morphological variables studied. Regression coefficients and $R^2$ values for each of these plots are provided in Table 2.

**Table 3**

Regression coefficients, $R^2$ values, and beta weights from multivariate regression analyses of the morphological variables studied. Only regression coefficients with $P < 0.10$ are provided.

| Variable[a] | Regression Coefficients | | | | | $R^2$ | Beta weights | | | |
|---|---|---|---|---|---|---|---|---|---|---|
| | Precip.[b] | Depth | Clay | Sand | Intercept | | Precip. | Depth | Clay | Sand |
| OC | 0.0174 | -0.036 | 0.0845 | - | - | 0.762 | 0.384 | -0.690 | 0.200 | 0.107 |
| BD | 0.0050 | 0.004 | -0.0256 | - | 1.01 | 0.567 | 0.756 | 0.481 | -0.413 | -0.032 |
| L* | -0.0370 | 0.195 | - | - | 23.76 | 0.723 | -0.173 | 0.797 | 0.026 | -0.159 |
| a* | - | 0.046 | - | -0.026 | 2.91 | 0.686 | 0.091 | 0.715 | -0.021 | -0.210 |
| b* | - | 0.128 | - | -0.072 | 6.42 | 0.754 | 0.092 | 0.756 | -0.047 | -0.220 |
| $COC_{0.163}$ | 0.0116 | -0.021 | 0.0722 | - | - | 0.871 | 0.419 | -0.673 | 0.280 | 0.029 |
| $COC_{0.1}$ | 0.0047 | -0.006 | 0.0728 | - | - | 0.818 | 0.318 | -0.344 | 0.527 | -0.084 |

[a] OC = organic carbon; BD = bulk density; COC = complexed organic carbon. Subscripts indicate which OC:clay threshold was used when calculating COC. Dexter et al. (2008) proposed the use of 0.1 as the treshold; 0.163 was found in this study.

[b] Precip. = precipitation.

regressions allowed for: (1) assessment of the amount of variation explained in each morphological property; (2) determination of significant predictor variables for each property; (3) examination of the direction of the correlations with each predictor variable; (4) comparison of the strength of the correlations among the morphological properties; and (5) creation of pedotransfer functions (PTFs: empirical prediction equations) for the properties studied.

Statistical analyses (not shown) of a range of independent variables including precipitation timing, magnitude, and average precipitation during the growing season, indicated that average annual precipitation, depth, clay, and sand display the least covariance and explain the largest portions of the dependent soil development indicators considered. All precipitation variables considered explain the variation in OC data when coupled with depth and texture variables; however, they show high covariance. Therefore, average annual precipitation was selected as it provided a slightly higher $R^2$-value. Predicted values were plotted against measured values (Fig. 12) using the multiple linear regression equations in Table 3 to assess the model fits. In addition, multivariate regressions were run on the *z*-score transformed variables to obtain the beta weights (i.e., partial regression coefficients) in order to compare the explanatory power among precipitation, depth, and PSD for each morphological property following Kachigan (1982) (Table 3).

Organic carbon is well explained ($R^2 = 0.762$) by average annual precipitation, depth, and clay content, especially for OC values less than 1.5% (Fig. 12). Squares of the beta weights in Table 3 indicate that depth is the strongest predictor for OC explaining 3.2 and 12 times the variation compared to precipitation and clay content, respectively (Table 3). As expected, depth is negatively correlated with OC while precipitation and clay content were positively correlated (Table 3). For COC using the OC:clay ratio from Dexter et al. (2008) of 0.1 ($COC_{0.1}$), the

multivariate regression is able to explain most of the range of COC values found in this study (Fig. 12). However, the quality of the prediction becomes less pronounced below COC values of 1%. As with OC, $COC_{0.1}$ displays both significant coefficients and correlations in the same direction for average annual precipitation, depth, and clay content. The major difference is that clay is the strongest predictor of $COC_{0.1}$. Clay content explains 2.4 and 2.8 times the variation in $COC_{0.1}$ compared to depth and precipitation, respectively. The reason clay content is able to explain more variation than the other independent variables is likely due to the low OC:clay threshold (i.e., 0.1), which allows clay to artificially limit the amount of OC complexed. By contrast, using a threshold of 0.163 ($COC_{0.163}$) determined from the broken stick analysis of the GMS measurements, clay is capable of explaining only a fraction of the variation compared to precipitation (44%) and depth (17%) as indicated by the square of the beta weights in Table 3. The multivariate model for $COC_{0.163}$ is able to explain 87.1% of the variation and performs better than either OC or $COC_{0.1}$ over the range of values measured. $COC_{0.163}$ is better explained ($R^2$ = 0.871) by the predictor variables (i.e., average annual precipitation, depth, and clay) than OC ($R^2$ = 0.762). This suggests that $COC_{0.163}$ is more responsive to pedogenesis along this climosequence than OC. The investigators are unaware of any studies that have documented COC changes along a precipitation gradient. To the extent that this finding can be extended, this COC climosequence indicates that loess soil physical quality with depth can be predicted, in part, by knowledge of average annual precipitation. Additionally, the improvement of the model fit for $COC_{0.163}$ compared to $COC_{0.1}$ further confirms that the 0.163 OC:clay ratio better represents microaggregation in the loess soils investigated in this study.

In addition to OC and COC, average annual precipitation is a significant predictor of bulk density and soil lightness (L*) (Fig. 12; Table 3). Precipitation explains 2.5 and 3.4 times the

variation in bulk density compared to depth and clay content, respectively (Table 3), indicating that precipitation strongly affects bulk density along the transect. The positive correlation between precipitation and bulk density indicates that total porosity in soils along the transect decreased under more humid conditions toward the east as observed in bulk density values (Fig. 4). A connection between porosity and precipitation suggests that soil physical quality changes along this precipitation gradient. This change, however, follows the reverse trend observed with the $COC_{0.163}$ data, perhaps indicating that while microaggregation increased toward the east end of the transect, macroaggregation increased toward the west. Given the small diameter of the cores used in this study this hypothesis, however, was not testable.

Depth was the most important variable determining lightness, explaining 21 and nearly 1000 times more variation than either precipitation or clay content, respectively (Table 3). Soil redness (a*) and yellowness (b*) are both significantly predicted from depth and sand content alike, which explains 68.6 and 75.4% of the variation, respectively (Fig.12; Table 3). The PTFs for these variables along with the OC, bulk density, and COC are provided in Table 3.

# CHAPTER 5. CONCLUSIONS

This research sought to explain the variability of morphological properties in soils developed within loess as a function of average annual precipitation in the Central Great Plains of the United States. Results indicate that color variables are least impacted by average annual precipitation: although the precipitation variable is significantly correlated to lightness (L*) values, depth within the soil cores is far more important in explaining variation in lightness. Redness (a*) and yellowness (b*) are not significantly impacted by average annual precipitation. PSD throughout the transect is relatively consistent, exhibiting a slight increase in silt and decrease in sand content from west to east with clay consistently around 10%, a relationship documented for the region by Muhs et al. (2008). SOC values decrease exponentially with depth at all sites, displaying a positive asymptotic correlation between OC and average annual precipitation throughout the upper 50 cm. This trend is especially pronounced in the 0 – 10 cm depth interval, indicating that the effects of average annual precipitation are most strongly expressed nearest the surface. The asymptotic trend indicates that a greater response in OC to increasing total annual precipitation should be expected for soils with drier climatic regimes (i.e., $<75$ cm $yr^{-1}$). In the multivariate analyses, depth was the strongest predictor for OC, explaining 3.2 and 12 times the variation compared to precipitation and clay content, respectively. With one exception, the eastern sites show increasing aggregation with depth, and, in general, variability in aggregation with depth decreases from west to east along the transect. The GMS proxy used in this study to represent aggregation when plotted against the OC:clay ratio provided a breakpoint of 0.163, suggesting that below this threshold organic carbon is complexed with clay to form soil microaggregates. Thus, in the relatively undisturbed, silt-dominated loess soils used in this study, every 1 g of OC is complexed with approximately 6 g of clay. COC values show a generally

linear decrease with depth for all sites and increase from west to east for all depth intervals. Total COC is highly correlated with average annual precipitation ($r^2$ = 0.938), indicating that the depth-wise physical qualities of loess-derived soils can be predicted, in part, by knowledge of average annual precipitation. Using the OC:clay threshold of 0.163, COC is somewhat better explained ($R^2$ = 0.871) by the predictor variables (i.e., average annual precipitation, depth, and clay) in the multivariate analyses than OC ($R^2$ = 0.762). This suggests that $COC_{0.163}$ is more responsive to pedogenesis along this climosequence than OC, and in turn that regional precipitation changes due to global climate forcings may contribute to a change of soil physical quality in the upper 50 cm. The improvement of the model fit for $COC_{0.163}$ compared to $COC_{0.1}$ further confirms that the 0.163 OC:clay ratio best represents microaggregation in the loess soils investigated in this study. Precipitation was the best predictor of bulk density. The positive correlation between precipitation and bulk density indicates that total porosity in soils decreases under the more humid conditions toward the east. This relationship, however, follows the reverse trend observed with the $COC_{0.163}$ data, perhaps indicating that, while microaggregation increases toward the east end of the transect, macroaggregation increases toward the west.

## REFERENCES


Arrouays, D., Pelissier, P., 1994. Modeling carbon storage profiles in temperate forest humic loamy soils of France. Soil Science 157, 185-192.

Bernoux, M., Arrouays, D., Cerri, C. C., Bourennane, H., 1998. Modeling vertical distribution of carbon in oxisols of the western Brazillian Amazon (Rondonia). Soil Science 163, 941-951.

Bettis, E. A. III, Muhs, D. R., Roberts, H. M., Wintle, A. G., 2003. Last glacial loess in the conterminous USA. Quaternary Science Reviews 22, 1907-1946.

Blake, G.R., Hartge, K.H., 1986. Bulk density. In: Klute, A. (Ed.), Methods of Soil Analysis, Part 1, Agronomy Monograph 9, 2nd edition. Agronomy Society of America, Soil Science Society of America, Madison, WI, pp. 363-374.

Brye, K. R., West, C. P., Gbur, E. E., 2004. Soil quality differences under native tallgrass prairie across a climosequence in Arkansas. The American Midland Naturalist 152, 214-230.

Burke, I. C., Yonker, C. M., Parton, W. J., Cole, C. V., Schimel, D. S., Flach, K., 1989. Texture, climate, and cultivation effects on soil organic matter content in U.S. Grassland soils. Soil Science Society of America Journal 53, 800-805.

Burt, R. (Ed.), 2004. Soil Survey Laboratory Methods Manual, Ver. 4.0, Soil Survey Investigations Report No. 42. Natural Resources Conservation Service, Washington, D.C.

Combs, S. M., Nathan, M. V., 1998. Soil organic matter. In: Brown, J. R. (Ed.), Recommended Chemical Soil Test Procedures for the North Central Region, North Central Regional Research Publication No. 221 (Revised), Missouri Agricultural Experiment Station, Columbia, MO. pp. 53-58.

Comission Internationale de l'Eclairage. 1978. Recommendations on uniform color spaces, color difference and psychometric color terms. Suppl. No. 2 to Publ. no 15, Colorimetry, CIE 1971, Paris.

de Jonge, L. W., Moldrup, P., Schjønning, P., 2009. Soil infrastructure, interfaces & translocation processes in inner space ("soil-it-is"): towards a road map for the constraints and crossroads of soil architecture and biophysical processes. Hydrology and Earth System Sciences 13, 1485-1502.

Dexter, A. R., 2004. Soil physical quality, Part I: theory, effects of soil texture, density, and organic matter, and effects on root growth. Geoderma 120, 201-214.

Dexter, A. R., Richard, G., Arrouays, D., Czyz, E. A., Jolivet, C., Duval, O., 2008. Complexed organic matter controls soil physical properties. Geoderma 144, 620-627.

Eden, M., Moldrup, P., Schjønning, P., Vogel, H. J., Scow, K. M., de Jonge, L. W., 2012. Linking soil physical parameters along a density gradient in a loess-soil long-term experiment. Soil Science 177, 1-11.

Hontoria, C., Saa, A., Rodríguez-Murillo, J. C., 1999. Relationships between soil organic carbon and site characteristics in peninsular Spain. Soil Science Society of America Journal 63, 614-621.

Jackson, R. B., Canadell, J., Ehleringer, J. R., Mooney, H. A., Sala, O. E., Schulze, E. D., 1996. A global analysis of root distributions for terrestrial biomes. Oecologia 108, 389-411.

Jacobs, P. M., Mason, J. A., 2005. Impact of Holocene dust aggradation on A horizon characteristics and carbon storage in loess-derived Mollisols of the Great Plains, USA. Geoderma 125, 95-106.

Jobbágy, E. G., Jackson, R. B., 2000. The vertical distribution of soil organic carbon and its relation to climate and vegetation. Ecological Applications 10, 423-436.

Johnson, W. C., Klopfenstein, S. T., 2013. Pioneer Cemetery Distribution within Kansas, ver. 1.0: Kansas Geological Survey, Data Access and Support Center. http://www.kansasgis.org/catalog/index.cfm

Kachigan, S. K., 1982. Multivariate Statistical Analysis: A conceptual Introduction. Radius Press, New York.

Khormali, F., Kehl, M., 2011. Micromorphology and development of loess-derived surface and buried soils along a precipitation gradient in Northern Iran. Quaternary International 234, 109-123.

Koch, G. W., Vitousek, P. M., Steffen, W. L., Walker, B. H., 1995. Terrestrial transects for global change research. Vegetatio 121, 53-65.

Muggeo, V. M. R., 2008. Segmented: An R package to fit regression models with broken-line relationships. R News 8, 20.

Muhs, D. R., Bettis, E. A. III, Aleinikoff, J. N., McGeehin, J. P., Beann, J., Skipp, G., Marshall, B. D., Roberts, H. M., Johnson, W. C., Benton, R., 2008. Origin and paleoclimatic significance of late Quaternary loess in Nebraska: Evidence from stratigraphy, chronology, sedimentology, and geochemistry: Geological Society of America Bulletin 120, 1378-1407.

Saiz G., Bird, M. I., Domingues, T., Schrodt, F., Schwarz, M., Feldpausch, T. R., Veenendaal, E., Djagbletey, G., Hien, F., Compaore, H., Diallo, A., Lloyd, J., 2012. Variation in soil carbon stocks and their determinants across a precipitation gradient in West Africa. Global Change Biology 18, 1670-1683.

Sala, O. E., Parton, W. J., Joyce, L. A., Lauenroth, W. K., 1988. Primary production of the central grassland region of the United States. Ecology 69, 40-45.

Schjønning, P., de Jonge, L. W., Munkholm, L. J., Moldrup, P., Christensen, B. T., Olesen, J. E., 2012. Clay dispersibility and soil friability—testing the soil clay-to-carbon saturation concept. Vadose Zone Journal 11. doi:10.2136/vzj2011.0067

Schulze, E. D., Mooney, H. A., Sala, O. E., Jobbagy, E., Buchmann, N., Bauer, G., Canadell, J., Jackson, R. B., Loreti, J., Oesterheld, M., Ehleringer, J. R., 1996. Rooting depth, water availability, and vegetation cover along an aridity gradient in Patagonia. Oecologia 108, 503-511.

Tan, Z. X., Lal, R., Smeck, N. E., Calhoun, F. G., 2004. Relationships between surface soil organic carbon pool and site variables. Geoderma 121, 187-295.

Torrent, J., Barrón, V., 1993. Laboratory measurement of soil color: theory and practice. In: Bingham, J.M., Ciolkosz, E.J. (Eds.), Soil Color. Soil Science Society of America, Madison, WI, pp. 21-33.

Zhou, X., Talley, M., Luo, Y., 2009. Biomass, litter, and soil respiration along a precipitation gradient in southern Great Plains, USA. Ecosystems 12, 1369-1380.